

## N O T I C E

THIS DOCUMENT HAS BEEN REPRODUCED FROM  
MICROFICHE. ALTHOUGH IT IS RECOGNIZED THAT  
CERTAIN PORTIONS ARE ILLEGIBLE, IT IS BEING RELEASED  
IN THE INTEREST OF MAKING AVAILABLE AS MUCH  
INFORMATION AS POSSIBLE

"Made available under NASA sponsorship  
in the interest of early and wide dis-  
semination of Earth Resources Survey  
Program information and without liability  
for any use made thereof."

SDSU-RSI-80-01

80-10075  
CR-162646

HCMM ENERGY BUDGET DATA AS A MODEL INPUT FOR ASSESSING  
REGIONS OF HIGH POTENTIAL GROUNDWATER POLLUTION

(E80-10075) HCMM ENERGY BUDGET DATA AS A MODEL INPUT FOR ASSESSING REGIONS OF HIGH POTENTIAL GROUNDWATER POLLUTION Interim Report, Oct. - Dec. 1979 (South Dakota State Univ.) 59 p HC A04/MF A01 CSCL 13B G3/43 N80-18524 Unclas 00075

Principal Investigator: Donald G. Moore

Report Author: J.L. Heilman

December 1979

Interim Type II Report for October-December, 1979

Prepared for:

Goddard Space Flight Center  
Greenbelt, Maryland 20771

RECEIVED

JAN 25 1980

SIS/902.6

HCMM032  
TYPE II

A. Problems

CCT's for scene I.D. numbers AA0125-08340, AA0131-19420, and A0040-08550 have not been received.

B. Accomplishments

Analyses has begun of digital data which have been received.

C. Significant Results

Significant results to date are summarized in Appendices, A, B and C. Appendix A is the revised version of a manuscript dealing with a ground study which appeared in the December 1978 progress report no. SDSU-RSI-79-01 and has been accepted for publication in Journal of Applied Meteorology. Appendix B, a manuscript submitted to Remote Sensing of Environment, describes detection of high soil moisture areas which was initially reported in the December 1978 report. Appendix C is a paper presented at the Fifth Pecora Symposium on satellite hydrology. It described, in part, HCMM detection of apparent thermal anomalies related to perched water tables. The apparent anomalies were detected on late-summer night IR imagery, but not on visible or day IR imagery. These results are consistent with earlier aircraft investigations.

D. Publications

See Appendices A, B and C.

E. Recommendations

None at this time.

F. Funds Expended

\$76,509.22

APPENDIX A

Thermography for Estimating Near-Surface Soil Moisture Under Developing  
Crop Canopies.

(To be published in March 1980 issue of Journal of Applied Meteorology)

1 THERMOGRAPHY FOR ESTIMATING NEAR-SURFACE SOIL  
2 MOISTURE UNDER DEVELOPING CROP CANOPIES<sup>1/</sup>

3 J.L. Heilman and D.G. Moore

4 Remote Sensing Institute

5 South Dakota State University

6 Brookings, South Dakota 57007  
7  
8  
9  
10  
11  
12  
13  
14  
15  
16  
17  
18  
19  
20  
21  
22

23  
24 <sup>1/</sup> Contribution no. SDSU-RSI-J-79-11 from the Remote Sensing Institute,  
25 South Dakota State University. This investigation was supported by  
26 NASA under Contract no. NAS5-24206 and the State of South Dakota.  
27

1  
2  
3  
4  
5  
6  
7  
8  
9  
10  
11  
12  
13  
14  
15  
16  
17  
18  
19  
20  
21  
22  
23  
24  
25  
26  
27

ABSTRACT

Previous investigations of thermal-infrared techniques using remote sensors (thermography) for estimating soil water content have been limited primarily to bare soil. Ground-based and aircraft investigations were conducted to evaluate the potential for extending the thermography approach to developing crop canopies. A significant exponential relationship was found between the volumetric soil water content in the 0 to 4-cm soil layer and the diurnal difference between surface soil temperature measured at 0230 and 1330 local standard time (satellite overpass times of NASA's Heat Capacity Mapping Mission HCMM). Surface soil temperatures were estimated using minimum air temperature, percent cover of the canopy and remote measurements of canopy temperature. Results of the investigation demonstrated that thermography can potentially be used to estimate soil temperature and soil moisture throughout a complete growing season for a number of different crops and soils.

ORIGINAL PAGE IS  
OF POOR QUALITY

1 1. Introduction

2 Remotely sensed surface temperatures have been investigated for  
3 estimating soil water content (Idso et al., 1975; Idso and Ehler, 1976;  
4 Schmugge et al., 1978). Soil water contents have been related to  
5 differences between the daily maximum and minimum soil or crop tempera-  
6 tures and air temperature. The investigations have generally been  
7 limited to bare soils or fully developed crop canopies because of  
8 difficulties in interpreting thermal data at less than full cover when  
9 significant emittance contributions from both soil and vegetation occur.  
10 The ability to derive useful information from remote temperature  
11 measurements for conditions other than bare soil or fully developed  
12 canopies would greatly expand the usefulness of the remote sensing  
13 techniques.

14 Investigators have shown that, even at full cover, thermal  
15 emittance from the soil surface can affect remote temperature measure-  
16 ments of crop canopies (Blad and Rosenberg, 1976).  
17 Thus, surface soil temperatures can potentially be estimated from  
18 remote measurements of land surface emittance where a crop canopy is  
19 the primary source of radiation.

20 We conducted a ground based and aircraft investigation to evaluate  
21 the potential for estimating soil surface temperature and soil moisture  
22 from measurements of total area emittance at various stages of crop  
23 canopy development. The investigation was conducted to examine data  
24 collected during times of the diurnal temperature cycle corresponding to  
25 data collection by NASA's Heat Capacity Mapping Mission (HCMM), launched  
26 in April 1978. The satellite, which carries a two-channel radiometer  
27 (0.5 to 1.1 and 10 to 12  $\mu\text{m}$ ) in a sun-synchronous orbit, collects data

1 at mid-latitudes at approximately 0230 and 1330 local standard time  
2 (LST) during the diurnal cycle with repeat coverage of five or 16 days  
3 depending on latitude.

## 4 2. Materials and Methods

### 5 Plot Study

6 Experiments were conducted on a 25 x 300-m field of Volga loam  
7 (fine, loamy over sandy, mixed (calcareous), frigid, Cumulic  
8 Haplaquoll) at the South Dakota State University Agricultural Engineer-  
9 ing Research Farm located 8-km south of Brookings, South Dakota. Larker  
10 barley (Hordeum vulgare L.) was planted in the field at 15-cm row  
11 spacings (north-south rows) and a population of 2.5 million plants/ha.  
12 Rainfall in the Brookings area averages 558 mm/year. No supplemental  
13 water was applied to the barley. Surface roughness of the soil was  
14 minimal.

15 Surface soil temperatures (about 1 mm below the soil surface) were  
16 measured with copper-constantan thermocouples at two locations (A and  
17 B) within the field. For each location, three thermocouples were wired  
18 in parallel to obtain an average measurement which approximated surface  
19 temperature. Apparent canopy temperatures consisting of emittance  
20 contributions from the soil surface and the barley (shaded and sunlit  
21 leaves) were measured with a portable infrared radiometer (Model PRT-5,  
22 Barnes Engineering Co.) at a vertical position (zero degree look angle  
23 measured from nadir) at a height of 2 m above the canopy. The  
24 temperature resolution of the 20 degree field of view PRT-5 was  $\pm 0.5^\circ \text{C}$   
25 in the 8 to 14  $\mu\text{m}$  wavelength interval. Apparent crop temperatures were  
26 measured with the PRT-5 at a height of 1 m above the canopy and a look  
27 angle of about 60 degrees to minimize emittance contributions from the

1 soil. Temperatures were measured at 0230 and 1330 LST.

2 The temperatures measured with the PRT-5 were not corrected for  
3 emissivity. Emissivities, determined using a procedure similar to that  
4 described by Fuchs and Tanner (1966), ranged from 0.96 for bare, dry  
5 soil to 0.98 for the fully developed barley canopy. For the range of  
6 temperatures and percent cover encountered, the maximum error from not  
7 correcting for emissivity was 1.5° C.

8 Soil water contents (0 to 4-cm layer) for each location were  
9 determined gravimetrically on soil samples collected at the time of the  
10 temperature measurements. The average of soil water contents measured  
11 at 0230 and 1330 LST was used to represent the 24-hour average. Jackson  
12 et al. (1976) reported that the average of the daily maximum and minimum  
13 water content closely approximated the 24-hour average.

14 Temperature and soil water content measurements were initiated when  
15 the canopy cover reached 30 percent. Data were collected for 22 dates  
16 during the 45-day investigation.

17 Plant samples for determining leaf area index (leaf area/soil area)  
18 were taken every five to seven days. Leaf areas (green leaves only)  
19 were measured with an optical planimeter (Lambda Instrument Corp.).  
20 Percent cover was determined using 35-mm color infrared slides of the  
21 canopy (photographed from a vertical position approximately one meter  
22 above the canopy) projected on a random dot grid. Daily values of leaf  
23 area index (LAI) and percent cover were estimated from graphs of  
24 observed LAI and percent cover versus date (Fig. 1). We did not  
25 estimate percentages of shaded and sunlit leaves, or percentages of  
26 shaded and sunlit soil.

27 Maximum and minimum air temperatures were obtained from the

ORIGINAL PAGE IS  
OF POOR QUALITY

1 Brookings National Weather Service Station (approximately 12 km from the  
2 research site). All data were subjected to regression analyses.

### 3 Aircraft Study

4 Apparent canopy temperatures of corn, soybean, millet, and pasture  
5 were collected along a 24-km flight line northwest of Brookings by a  
6 quantitative thermal scanner (Daedalus Enterprises, Inc., Ann Arbor,  
7 Michigan) flown in the Remote Sensing Institute's twin engine Beechcraft  
8 at an altitude of 3650 m above ground level. The temperature resolution  
9 of the scanner was 0.5° C, and the spatial resolution was 16-cm per  
10 100 m of altitude at nadir. Data were collected at 1330 and 0230 LST  
11 on September 5 and 6, 1978. Scanner data were not corrected for  
12 atmospheric attenuation or emissivity variations. Sky conditions were  
13 clear for all flights. Errors from neglecting emissivity variations  
14 and atmospheric effects were less than 1° C.

15 Soil water contents (0 to 4-cm layer) were gravimetrically sampled  
16 in each of the fields at the time of the aircraft overflights. Percent  
17 cover was estimated using the same procedure used in the plot study.  
18 Data from the aircraft study were used to test the predictive equations  
19 developed from the plot study on barley.

## 20 3. Results and Discussion

### 21 Soil Water Content Versus Temperature Relationships

22 The amplitude of the diurnal soil surface temperature wave is a  
23 function of thermal inertia and meteorological factors (solar radiation,  
24 air temperature, humidity, etc.). Thermal inertia, an indication of a  
25 soil's resistance to temperature change, is defined as  $\rho c \lambda^{1/2}$  where  $\rho$  is  
26 density,  $c$  is specific heat, and  $\lambda$  is thermal conductivity. Since  $\rho$ ,

c and  $\lambda$  of a soil increase as soil water content increases, the resulting amplitude of the diurnal temperature wave decreases.

When the soil surface is wet, evaporation is a major factor controlling surface heat loss. After the surface layer dries and the soil water supply cannot meet the evaporative demand, surface heat loss is by conductive transfer (soil heat flux) and is largely influenced by thermal inertia. Nocturnal cooling is highly related to thermal inertia. Thus, the diurnal surface temperature range can be an indication of soil water content. Idso et al. (1975) found a linear relationship between the diurnal range of surface soil temperatures and soil water content in the 0 to 4-cm layer of soil, and reported that the temperature versus water content relationship was a function of soil type. However, they also found that if soil water content was expressed in units of pressure potential, this dependence was minimal.

Vegetation cover alters the solar radiation at the soil surface and thus affects soil evaporation and soil temperatures. Therefore, dynamic growth and development of vegetation would be expected to complicate the temperature versus water content relationship.

Initially, we evaluated the relationship of day minus night surface soil temperatures ( $\Delta T_s$ ) versus soil water content at various stages of canopy development. Leaf area index and percent cover of the barley canopy ranged from 0.3 to 3.2 and 30 to 90 percent respectively. The exponential equation

$$\Delta T_s = e^{-0.06 \text{ SWC} + 3.59} \quad (1)$$

with an  $r^2$  of 0.81 and a standard deviation from regression of  $2.54^\circ \text{C}$  was found to best represent the relationship between  $\Delta T_s$  and the average 24-hr volumetric soil water content (SWC) in the 0 to 4-cm

ORIGINAL PAGE  
OF POOR QUALITY

1 layer of the soil profile (Fig. 2). The exponential form fit the data  
2 better than linear ( $r^2 = 0.71$ ), power ( $r^2 = 0.76$ ) or quadratic  
3 ( $r^2 = 0.77$ ) curves.

4 Idso et al. (1976) proposed a procedure for compensating for  
5 environmental variability in the thermal inertia approach by normalizing  
6  $\Delta T_s$  measurements with respect to an arbitrary standard diurnal air  
7 temperature variation. We found no significant improvement in the  $\Delta T_s$   
8 versus SWC relationship using the same normalization procedure.

9 The temperature versus water content relationship (Eq. 1) applies  
10 only to Volga loam. However, Idso et al. (1975) converted soil water  
11 content to a pressure potential and found a more universal relationship  
12 that appeared to be independent of soil type. Schmugge et al. (1978)  
13 reported that, in the absence of pressure potential data, textural  
14 differences in temperature versus water content relationships could be  
15 reduced by expressing soil water content as a percent of field capacity.  
16 The temperature versus soil water content relationships have limited  
17 usefulness unless soil temperatures can be estimated from remote  
18 measurements under all crop-cover conditions.

19 Estimating Soil Temperature from Measurements of Canopy Temperature

20 During the investigation, surface-soil temperatures at 0230 LST  
21 were 1.1 to 5.4° C higher than apparent crop (barley) temperatures,  
22 while PRT measurements of apparent canopy temperature (including crop  
23 and soil background) at 0230 LST were 1.1 to 2.2° C higher than apparent  
24 crop temperatures (Fig. 3a). Differences between canopy and crop  
25 temperatures, even at full cover, probably were the result of signifi-  
26 cant amounts of thermal radiation from the soil surface being detected  
27 by the infrared radiometer at 0230 LST (Blad and Rosenberg, 1976).

15

At 1330 LST, radiometric measurements of apparent canopy temperature were 0.5 to 17° C higher, and surface-soil temperatures 1.5 to 20° C higher, than apparent crop temperatures (Fig. 3b). Greatest differences between canopy and crop temperatures at full cover occurred on days with high temperatures and high evaporative demand. On those days, some wilting of leaves occurred, which exposed more of the soil background to incoming solar radiation.

Because emittance contributions from the soil surface apparently were detected by the infrared radiometer, equations were developed from regression analyses to estimate soil temperatures from remote measurements of canopy temperature. For the 0230 LST measurements, the equation

$$T_s(0230) = 0.40 \text{ PRT}_{(0230)} + 0.60 T_{a \text{ min}} + 5.10 \quad (2)$$

with an  $R^2$  of 0.78 and a standard deviation from regression of 1.31° C was obtained where  $T_s(0230)$  (°C) is surface soil temperature,  $\text{PRT}_{(0230)}$  (°C) is PRT measurement of canopy temperature, and  $T_{a \text{ min}}$  is the minimum NWS air temperature. For the 1330 LST measurement, the surface soil temperatures were related to the PRT measurements of canopy temperature and an exponential function of percent cover (PC). The equation

$$T_s(1330) = 0.79 \text{ PRT}_{(1330)} \times e^{(-0.80 \text{ PC})} + 20.35 \quad (3)$$

with an  $r^2$  of 0.86 and a standard deviation from regression of 2.63° C was obtained where PC is expressed as a fraction. We found no improvement in estimating soil temperature by including leaf area index, solar radiation, or maximum air temperature in the analyses. Figure 4 compares predicted soil temperature with observed values.

Measurements of canopy temperature used to derive (2) and (3)

1 ranged from 13 to 22° C for (2), and from 24 to 52° C for (3). Percent  
2 cover ranged from 0.3 to 0.9.

### 3 Evaluation of Results

4 Figure 5 compares observed soil water contents with values  
5 predicted using Eqs. (1) through (3), and the aircraft thermal scanner  
6 measurements of apparent corn, soybean, millet and pasture canopy  
7 temperatures. Equation (1) was converted to express soil water content  
8 as a percent of field capacity to minimize differences associated with  
9 soil texture (Schmugge et al., 1978). Percent canopy cover ranged from  
10 50 to 80 percent for pasture and from 90 to 95 percent for corn, soy-  
11 bean, and millet. Soil textures ranged from sandy loam to silty clay  
12 loam. Differences of observed from predicted values ranged from -24.5  
13 to +15.3 percent of field capacity. The average difference was 1.6  
14 percent of field capacity. The less accurate estimates of soil moisture  
15 for corn, soybean, and millet were probably due to the high percent  
16 cover.

### 17 4. Concluding Remarks

18 Results of this investigation indicate that thermography for  
19 estimating soil water content can potentially be extended to  
20 developing crop canopies. The diurnal difference between surface soil  
21 temperatures measured at HCMH overpass times is correlated with surface  
22 soil water content. Surface soil temperatures can be estimated from  
23 remote measurements of canopy temperature if minimum air temperature  
24 and percent cover of the canopy are known. Remote sensing evaluation  
25 of crop cover have been demonstrated (Heilman et al., 1977; Kanemasu  
26 et al., 1977; Tucker, 1979) for certain species.

ORIGINAL PAGE IS  
OF POOR QUALITY

1 5. Acknowledgements

2 We wish to thank Mr. W. Heilman for his assistance in data  
3 collection.

4

5

6

7

8

9

10

11

12

13

14

15

16

17

18

19

20

21

22

23

24

25

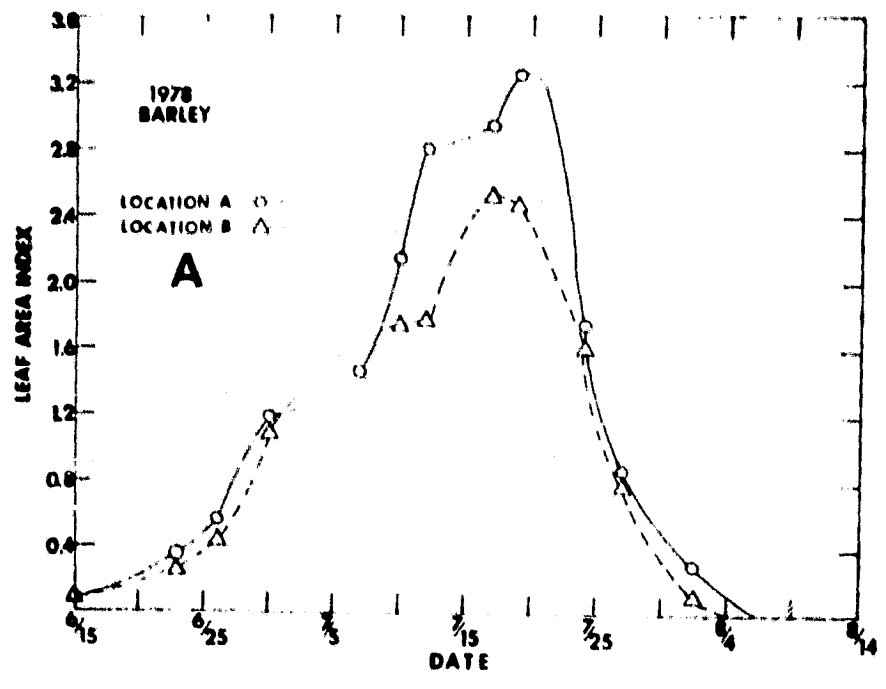
26

27

## REFERENCES

- 1
- 2 Blad, B.L. and N.J. Rosenberg, 1976: Measurement of crop temperature by  
3 leaf thermocouple, infrared thermometry and remotely sensed  
4 thermal imagery. *Agron. J.*, 68, 635-641.
- 5 Fuchs, M.E., and C.B. Tanner, 1966: Infrared thermometry of vegetation.  
6 *Agron. J.*, 58, 596-601.
- 7 Heilman, J.L., F.T. Kanemasu, J.O. Bagley, and V.P. Rasmussen, 1977:  
8 Evaluating soil moisture and yield of winter wheat in the Great  
9 Plains using Landsat data. *Remote Sensing of Environment*, 6,  
10 315-326.
- 11 Idso, S.B., T.J. Schmugge, R.D. Jackson, and R.J. Reginato, 1975: The  
12 utility of surface temperature measurements for the remote  
13 sensing of surface soil water status. *J. Geophys. Res.*, 80,  
14 3044-3049.
- 15 Idso, S.R. and W.L. Ehrlter, 1976: Estimating soil moisture in the root  
16 zone of crops: a technique adaptable to remote sensing. *Geophys.*  
17 *Res. Letters*, 3, 23-25.
- 18 Idso, S.B., R.D. Jackson, and R.J. Reginato, 1976: Compensating for  
19 environmental variability in the thermal inertia approach to  
20 remote sensing of soil moisture. *J. Appl. Meteor.*, 15, 811-817.
- 21 Jackson, R.D., R.J. Reginato, and S.B. Idso, 1976: Timing of ground  
22 truth data acquisition during remote assessment of soil-water  
23 content. *Remote Sensing of Environment*, 44, 249-255.
- 24 Kanemasu, E.T., J.L. Heilman, J.O. Bagley, and W.L. Powers, 1977:  
25 Using Landsat data to estimate evapotranspiration of winter wheat.  
26 *Environmental Management*, 1, 515-520.
- 27 Schmugge, T., B. Blanchard, A. Anderson, and J. Wang, 1978: Soil  
moisture sensing with aircraft observations of the diurnal  
range of surface temperature. *Water Resour. Bull.*, 14, 169-178.
- Tucker, C.J., 1979: Red and photographic infrared linear combination  
for monitoring vegetation. *Remote Sens. Environ.* (accepted)

ORIGINAL PAGE IS  
OF POOR QUALITY



ORIGINAL IS  
OF PUBLISHED QUALITY

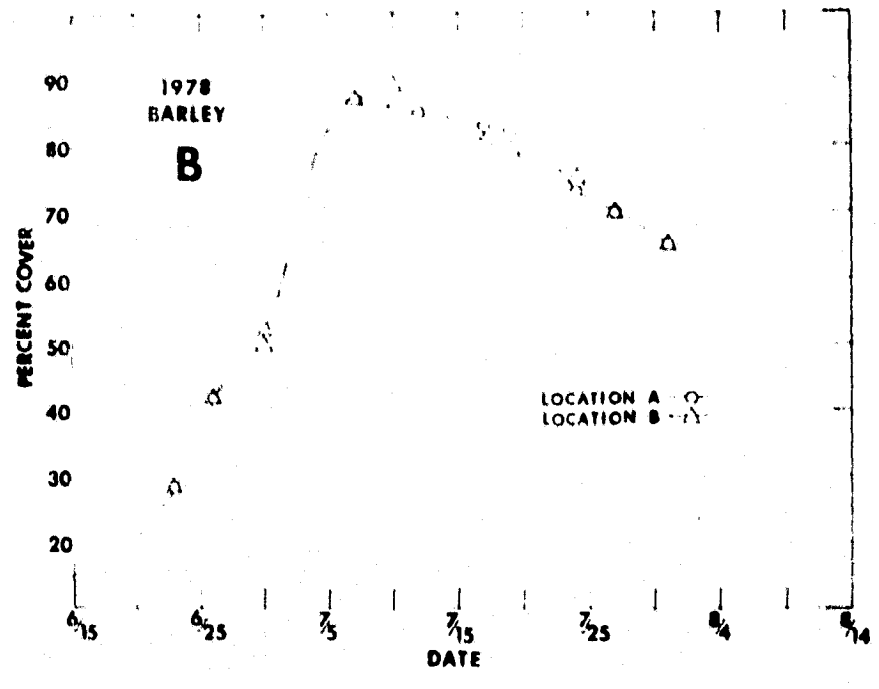


Fig. 1. Seasonal variations in leaf area index (A) and percent cover (B) of the barley canopy. Jointing and heading occurred on June 16 and July 19, respectively.

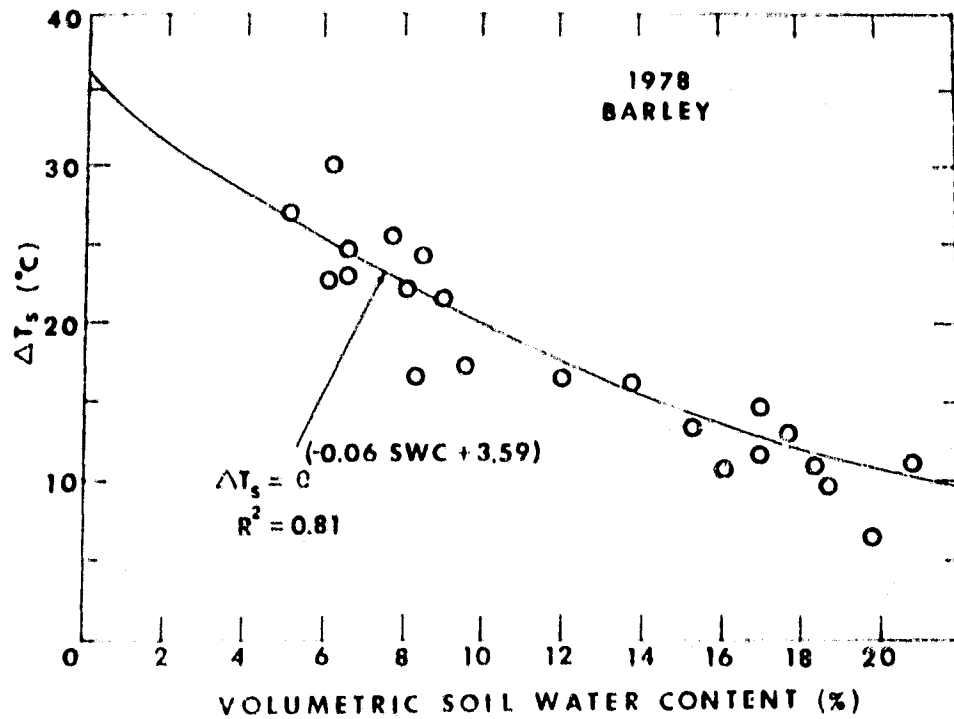


Fig. 2. Relationship of the difference ( $\Delta T_s$ ) between soil surface temperatures measured at 1330 and 0230 local standard time and the average 24-hr volumetric soil water content (SWC) in the 0 to 4-cm layer of the profile.

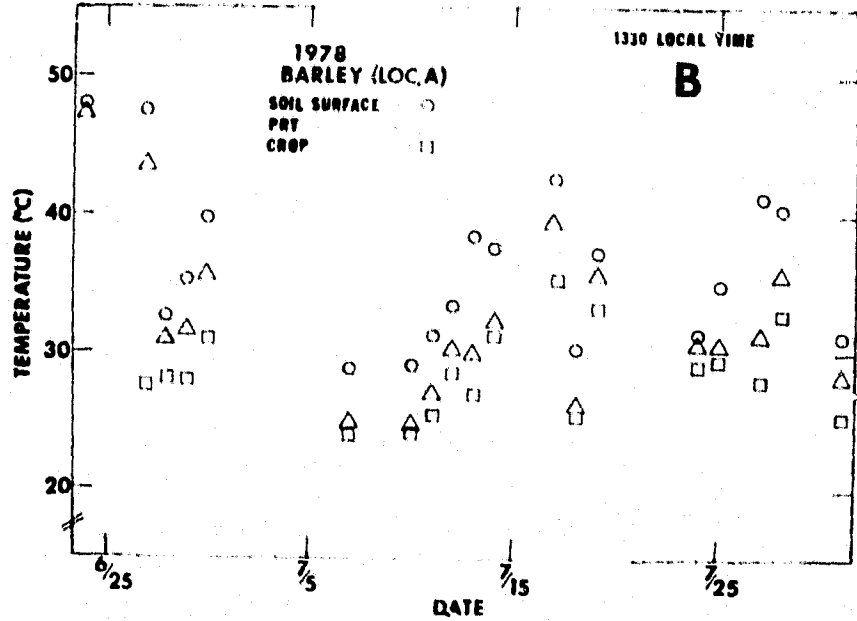
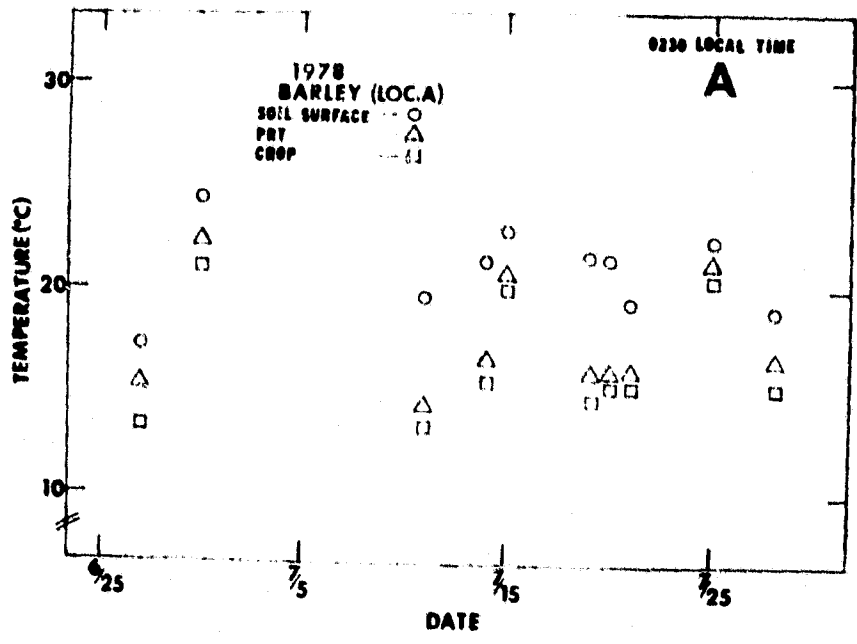


Fig. 3. Comparison of soil-surface (1-mm below surface), apparent canopy (PRT), and apparent crop temperatures measured at 0230 (A) and 1330 local standard time (B). Canopy temperatures included emittance contributions from the crop and soil background.

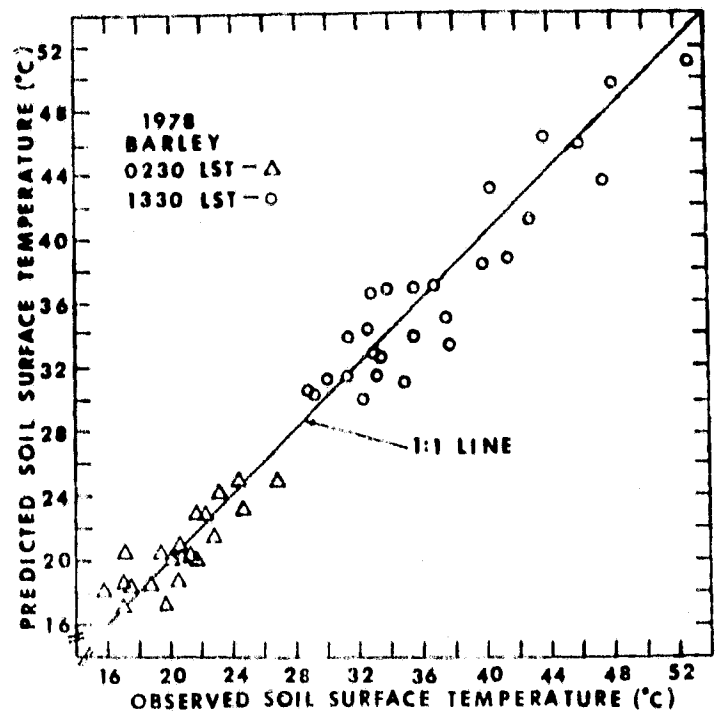


Fig. 4. Comparison of predicted and observed values of surface soil temperature at 0230 and 1330 local standard time (LST). Temperatures were predicted using equations (2) and (3).

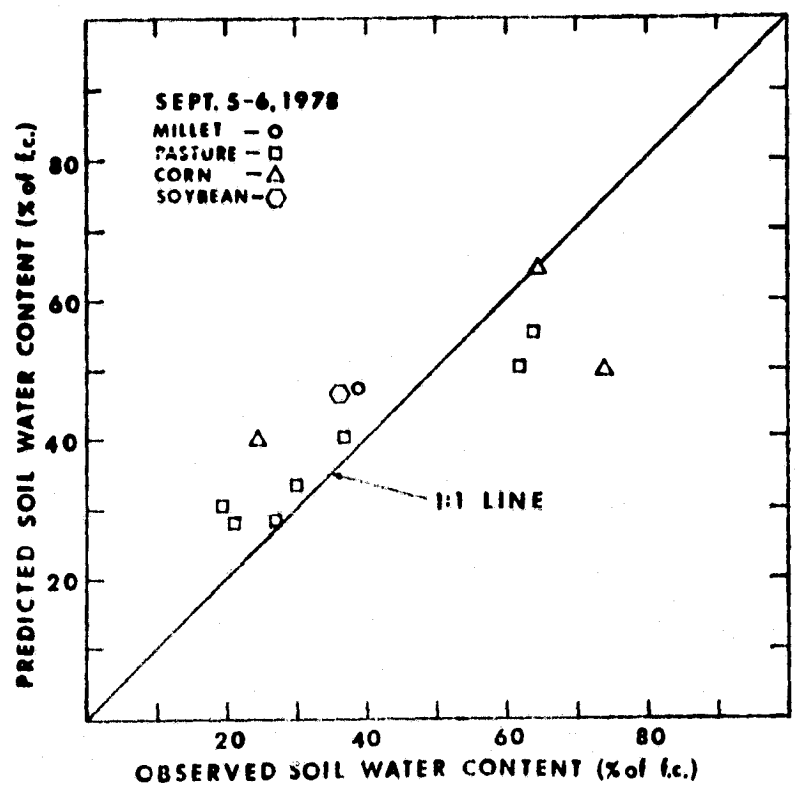


Fig. 5. Comparison of predicted and observed values of 24-hr average soil water content in the 0 to 4-cm layer of the soil profile. Predictions were made using equations (1), (2), and (3) and aircraft thermal scanner measurements of canopy temperature.

APPENDIX B

HCMM Detection of High Soil Moisture Areas

(Submitted as a short communication to Remote Sensing of Environment)

1  
2  
3  
4  
5  
6  
7  
8  
9  
10  
11  
12  
13  
14  
15  
16  
17  
18  
19  
20  
21  
22  
23  
24  
25  
26  
27

HCMM DETECTION OF HIGH SOIL MOISTURE AREAS<sup>1/</sup>

J.L. Heilman and D.G. Moore  
Remote Sensing Institute  
South Dakota State University  
Brookings, South Dakota 57007

ORIGINAL PAGE IS  
OF POOR QUALITY

<sup>1/</sup> Contribution No. SDSU-RSI-J-79-10 from the Remote Sensing Institute,  
South Dakota State University. Support was provided by NASA  
Contract No. NAS5-24206 and the State of South Dakota.

BACKGROUND

1  
2  
3  
4  
5  
6  
7  
8  
9  
10  
11  
12  
13  
14  
15  
16  
17  
18  
19  
20  
21  
22  
23  
24  
25  
26  
27

Thermal infrared detection and quantification of near-surface soil water content are based on relationships between surface soil temperature and soil moisture. Diurnal variations of surface soil temperature are related to soil thermal properties and meteorological factors such as solar radiation, air temperature, relative humidity, wind, etc. The meteorological factors represent the driving force for diurnal soil temperature variations. Thermal inertia ( $Jm^{-2} sec^{-1/2} K^{-1}$ ), defined as  $(\lambda C)^{1/2}$  where  $\lambda(Wm^{-1} K^{-1})$  is thermal conductivity and  $C(Jm^{-3} K^{-1})$  is volumetric heat capacity, represents a soil's resistance to the driving force. Since  $\lambda$  and  $C$  increase with an increase of soil moisture, the resulting range of surface soil temperature will decrease.

When the soil surface is wet, evaporation is a major factor controlling surface heat loss. As the surface layer dries and the soil water supply cannot meet the evaporative demand, soil temperature is largely influenced by thermal inertia. Thus, the diurnal range of surface soil temperature can be an indication of soil water content. Idso et al. (1975) found a significant relationship between the diurnal range of surface soil temperature (bare soil) and surface soil water content, and reported that the relationship was a function of soil type. Pratt and Ellyett (1979) presented a method for estimating soil thermal properties for changes in composition, porosity, and moisture content. Although temperature versus water content relationships are complicated by vegetation, Heilman et al. (1978) demonstrated the potential for estimating near-surface soil moisture from remote temperature measurements of crop canopies at incomplete cover.

One objective of NASA's Heat Capacity Mapping Mission (HCMM) is to

1 evaluate the feasibility of using HCMM data to assess soil moisture  
2 effects by observing temperatures near the maximum and minimum of the  
3 diurnal temperature cycle. The satellite, which carries a two-channel  
4 radiometer (0.5 to 1.1 and 10.5 to 12.5  $\mu\text{m}$ ), collects data at 1:30 p.m.  
5 and 2:30 a.m. local time at mid latitudes with a repeat cycle of 5 or  
6 16 days depending on latitude. Spatial resolutions are 0.5 x 0.5 km at  
7 nadir for the visible channel and 0.6 x 0.6 km at nadir for the thermal  
8 infrared channel. An example of HCMM detection of a region of high  
9 soil moisture is presented in the following discussion.

#### 10 DISCUSSION

11 In early April 1978 heavy runoff from snowmelt and ice blockage  
12 caused significant flooding of alluvial areas in a portion of the Big  
13 Sioux River Basin in southeastern South Dakota (Fig. 1). By mid-May,  
14 flood waters had receded, but an area of high soil moisture (at or near  
15 field capacity) remained. Soil moisture in the surrounding terrace  
16 soils was generally less than in the flood plain.

17 The high moisture area appeared warmer than surrounding areas on  
18 May 14 HCMM night thermal imagery (Fig. 2) and cooler than surrounding  
19 areas on May 15 HCMM day thermal imagery (Fig. 3). The temperature  
20 differences between alluvial and surrounding areas were probably the  
21 result of thermal inertia and evaporation differences associated with  
22 soil moisture differences. The high moisture area was not visible on  
23 Landsat imagery (Fig. 4).

24 Although digital data were not available at the time of the  
25 writing of this article to quantify radiometric temperature  
26 differences associated with the soil moisture differences, results  
27 presented here demonstrated the superiority of HCMM thermal data

1 acquired at the appropriate periods of the diurnal temperature cycle  
2 over Landsat data for assessing soil moisture differences. Final  
3 results from HCMM soil moisture investigations currently in progress  
4 will fully evaluate the utility of using HCMM and similar data for  
5 evaluating soil moisture from space.

6  
7  
8  
9  
10  
11  
12  
13  
14  
15  
16  
17  
18  
19  
20  
21  
22  
23  
24  
25  
26  
27

## REFERENCES

- 1  
2 Heilman, J.L., Moore, D.G., and Beutler, G. (1978), HCMM Energy Budget  
3 Data as a Model Input for Assessing Regions of High Potential  
4 Groundwater Pollution, Interim Report No. SDSU-RSI-78-01, Remote  
5 Sensing Institute, South Dakota State University, to Goddard  
6 Space Flight Center. Contract No. NAS5-24206.
- 7 Idso, S.B., Schmugge, T.J., Jackson, R.D., and Reginato, R.J. (1975),  
8 The Utility of Surface Temperature Measurements for the Remote  
9 Sensing of Soil Water Status, J. Geophys. Res., 80:3044-3049.
- 10 Pratt P.A., and Ellyett, C.D. (1979), The Thermal Inertia Approach  
11 to Mapping of Soil Moisture and Geology, Remote Sens. Environ.  
12 8:151-168.
- 13  
14  
15  
16  
17  
18  
19  
20  
21  
22  
23  
24  
25  
26  
27

LIST OF FIGURES

Figure

- 1 Landform map of Brookings County, South Dakota, showing location of alluvial soils (bottomland) of the Big Sioux River Basin which were flooded in early April 1978.
- 2 Photographic enlargement of a May 14, 1978, night thermal infrared image (scene ID A-A0018-08420) showing a high soil moisture area (arrows) in southeastern South Dakota. Dark is cool.
- 3 Photographic enlargement of a May 15, 1978, day thermal infrared image (scene ID A-A0029-19575) showing a high soil moisture area (arrows) in southeastern South Dakota. Dark is cool.
- 4 Photographic enlargement of a May 13, 1978, Landsat MSS 7 image (scene ID E-21207-16083) of the same area shown in Fig. 2 and 3.

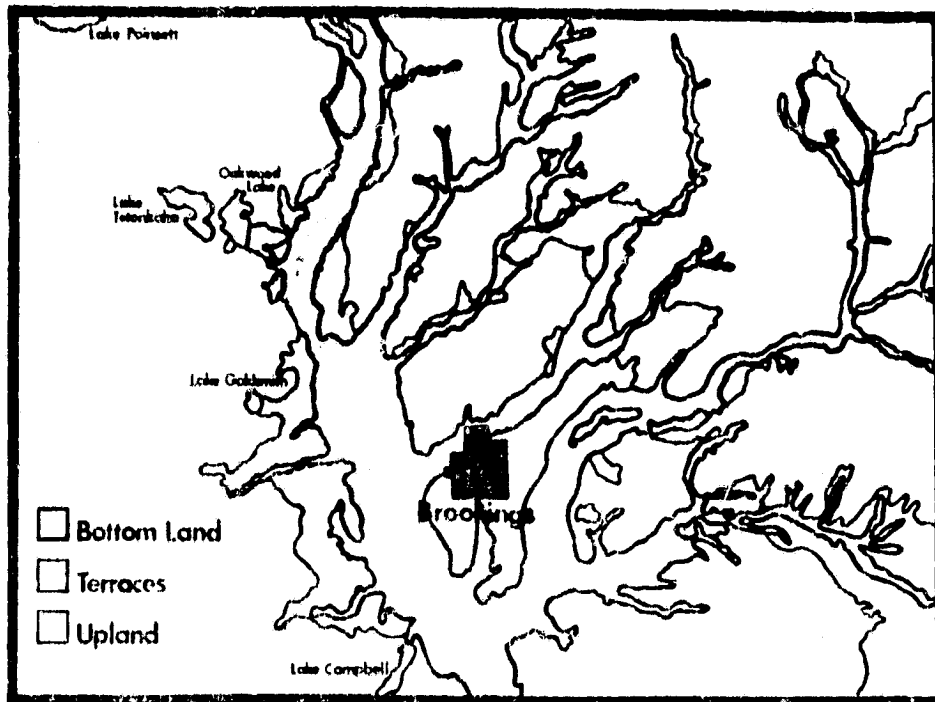


Fig. 1. Landform map of Brookings County, South Dakota, showing location of alluvial soils (bottomland) of the Big Sioux River Basin which were flooded in early April 1978.

UNIVERSAL ENERGY  
OF POOR QUALITY

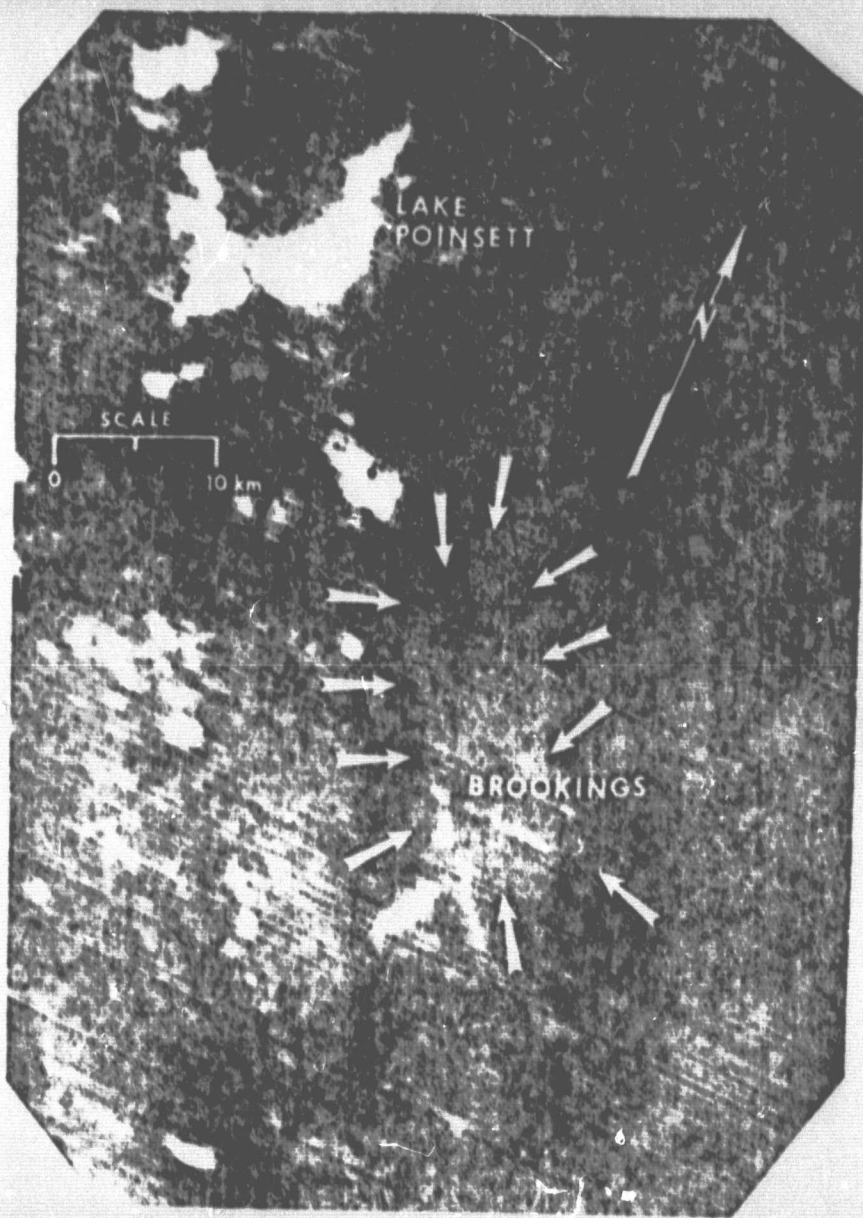


Fig. 2. Photographic enlargement of a May 14, 1978, night thermal infrared image (scene ID A-10018-08420) showing a high soil moisture area (arrows) in southeastern South Dakota. Dark is cool.

ORIGINAL PAGE IS  
OF POOR QUALITY

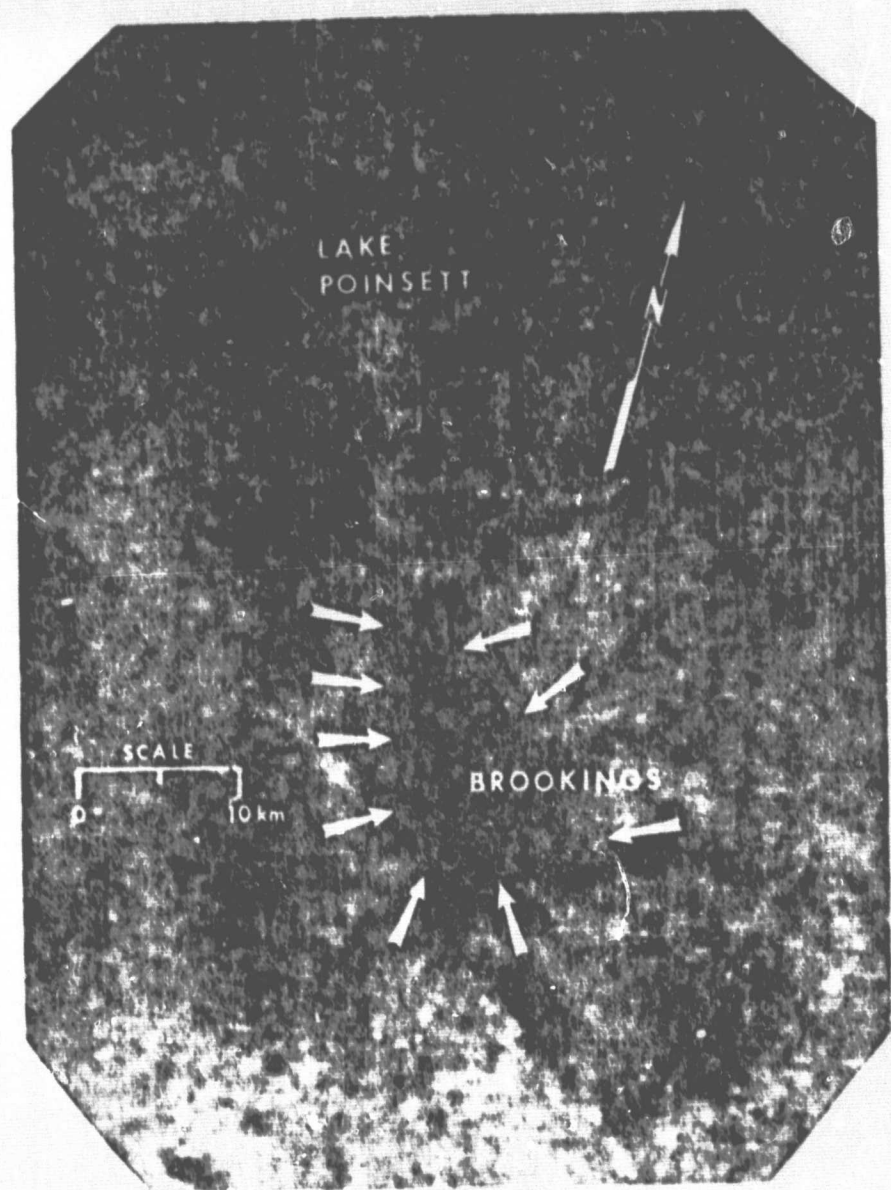


Fig. 3. Photographic enlargement of a May 15, 1978, day thermal infrared image (scene ID A-A0029-19575) showing a high soil moisture area (arrows) in southeastern South Dakota. Dark is cool.



Fig. 4. Photographic enlargement of a May 13, 1978, Landsat MSS 7 image (scene ID E-21207-16083) of the same area shown in Fig. 2 and 3.

ORIGINAL PAGE IS  
OF POOR QUALITY

APPENDIX C

Hydrologic Investigation of Eastern South Dakota Using HCMM Data

(To be published in Proceedings of Fifth Pecora Symposium on Satellite Hydrology)

HYDROLOGIC INVESTIGATION OF EASTERN  
SOUTH DAKOTA USING HCIM DATA

J.L. Heilman and D.G. Moore<sup>1/</sup>

---

<sup>1/</sup>Research Soil Physicist and Assistant Director, Remote Sensing Institute,  
South Dakota State University, Brookings, South Dakota 57007.

## ABSTRACT

Results of ground, aircraft, and satellite investigations are presented that demonstrate the potential for using data from NASA's Heat Capacity Mapping Mission (HCMM) satellite to provide information on near-surface soil moisture and perched water tables. The satellite, which carries a two-channel radiometer (0.5 to 1.1 and 10.5 to 12.5  $\mu\text{m}$ ) in a sun-synchronous orbit, collects data at approximately 0230 and 1330 local standard time with repeat coverage of five or 16 days depending on latitude. Perched water tables influence surface and subsurface soil temperatures because of a heat sink effect created by the high heat capacity of water. Near-surface soil moisture influences surface temperature through conductive heat transfer (affected by thermal inertia) and evaporation. Thus, HCMM data acquired near maximum and minimum periods of the diurnal temperature cycle can provide useful soil moisture information. Hydrologic interpretations of HCMM data are complicated by thermal inertia-heat sink interactions, vegetation, evapotranspiration, topography, atmospheric absorption and other environmental variables such as solar radiation, temperature, wind, etc.

KEY TERMS: HCMM, Thermal Inertia, Energy Balance, Soil Moisture, Groundwater

## INTRODUCTION

Virtually all physical processes occurring at the earth's surface or in the atmosphere involve transformations or transfers of energy. Energy balance interactions have important hydrologic implications since water and energy balances are intimately related (evapotranspiration requires a source of energy). Distribution of precipitation affects the thermal regime of the surface through changes in evapotranspiration and thermal properties of soil and vegetation. Surface temperatures are also influenced by distribution and flow of shallow aquifers.

Surface temperatures can provide information on the nature of surface and subsurface hydrology. However, spatial and temporal variations in surface temperature are difficult to evaluate on the ground. The spatial criterion can be fulfilled by remote sensing from aircraft and satellite. Monitoring of dynamic hydrologic features, such as soil moisture, which requires repetitive coverage is feasible only with satellites.

NASA's Heat Capacity Mapping Mission (HCMM) launched on April 26, 1978, is the first satellite designed to evaluate remote sensor-derived temperature measurements of the earth's surface at times when the temperature variation is at a maximum. Thus, the HCMM represents a potentially useful tool for hydrologic studies.

Ground, aircraft, and satellite investigations were conducted in eastern South Dakota to evaluate the potential for using HCMM data to monitor soil moisture and depth to shallow groundwater. Many of the results are preliminary since investigations are still in progress.

Eastern South Dakota is characterized by shallow perched water tables and significant spatial and temporal variations in soil moisture and agricultural land use. Most topographic features in the area are related to glaciation or stream erosion. The complexities of the groundwater regime and land use patterns in eastern South Dakota provide a wide range of conditions in which HCMM data can be evaluated.

#### HEAT CAPACITY MAPPING MISSION

The HCMM carries a two-channel radiometer (0.55 to 1.1 and 10.5 to 12.5  $\mu\text{m}$ ) in a sun-synchronous orbit (orbital altitude is 620 km). Spatial resolutions are 0.5 x 0.5 km at nadir for the visible channel and 0.6 x 0.6 km at nadir for the thermal infrared channel. The next of the thermal channel is 0.4°K at 280°K. Swath width is 716 km. HCMM collects data at 2:30 a.m. and 1:30 p.m. local standard time at mid-latitudes with a repeat cycle of five of 16 days depending on latitude.

Standard data products include visible, day IR, and night IR imagery (1:4,000,000 scale), and associated computer compatible tapes. An example of a night thermal IR image is shown in Fig. 1. Special data products include day-night temperature difference and apparent thermal inertia (ATI). ATI, which has many attributes of true thermal inertia, is defined as  $C(1-a)/\Delta T$  where C is a constant related to latitude and solar declination, a is apparent albedo obtained from daytime HCMM reflectivity measurements, and  $\Delta T$  is the day-night radiometric temperature difference observed by HCMM.

## INTERPRETATION EXAMPLES

Soil Moisture

Diurnal variations of surface soil temperatures are principally related to thermal inertia, evaporation, land use, and meteorological factors (solar insolation, air temperature, humidity, etc.). Thermal inertia, an indication of a soil's resistance to temperature change, is defined as  $(C\lambda)^{1/2}$  where  $C$  is volumetric heat capacity and  $\lambda$  is thermal conductivity. Since  $C$  and  $\lambda$  increase as soil water content increases, the resulting amplitude of the diurnal soil temperature wave decreases.

When the soil surface is wet, evaporation is a major factor controlling surface heat loss since less energy is partitioned into latent heat of vaporization and is not available for heating the soil. After the surface layer dries and the soil water supply cannot meet the evaporative demand, surface temperature of a bare soil is largely related to thermal inertia. Nocturnal cooling is highly dependent on thermal inertia. Thus, the amplitude of diurnal soil temperature variations can be an indication of near-surface soil water content.

Idso et al. (1975) found a linear relationship between the diurnal range of surface soil temperatures (bare soil) and near-surface soil water content, and reported that the temperature versus water content relationship was a function of soil type. The textural dependence can be minimized by expressing soil water content in units of pressure potential or as a percent of field capacity (Idso et al., 1975; Schmugge et al., 1978). Meteorological variability can be reduced

by normalizing the amplitude of the diurnal surface soil temperature wave with respect to a standard diurnal air temperature variation (Idso et al., 1976).

Vegetation alters solar insolation at the soil surface and thus affects soil temperature. Therefore, growth and development of vegetation would be expected to complicate temperature versus soil water content relationships. Since crop canopies are the primary source of land surface emittance during most of the growing season in South Dakota, the use of HCMM data for hydrologic investigations requires that vegetation be considered in the analysis.

A ground study was conducted in a barley canopy planted in a 25 x 300 m field of Volga loam to evaluate soil temperature (measured at HCMM overpass times by thermocouples 1-mm below the soil surface) versus water content relationships at various stages of canopy development (Heilman and Moore, 1979a). Percent cover of the developing barley canopy ranged from 30 to 90 percent over the 45-day study. The exponential equation

$$\Delta T_s = e^{(-0.06 \text{ SWC} + 3.59)} \quad (1)$$

with an  $r^2$  of 0.81 was found to best represent the relationship between day minus night surface soil temperatures ( $\Delta T_s$ ) and the average 24-hr volumetric soil water content (SWC) in the 0 to 4-cm layer of the soil profile (Fig. 2).

The relationship in (1) has limited usefulness unless  $\Delta T_s$  can be estimated from remote measurements under a wide range of crop-cover

conditions. The ground study found that apparent canopy temperatures measured 2 m above the canopy by a 20° FOV infrared radiometer (Model PRT-5, Barnes Engineering Co.) at a vertical position (zero degree look angle measured from nadir) at HCMM overpass times contained significant emittance contributions from both the soil and the crop canopy throughout the growing season. Therefore, equations were developed from regression analyses of surface-soil and apparent-canopy temperatures to estimate surface-soil temperature from remote measurements. For 0230 LST measurements, the equation

$$T_s(0230) = 0.40 T_c(0230) + 0.60 T_{a \text{ min}} + 5.10 \quad (2)$$

with an  $R^2$  of 0.78 was obtained where  $T_s(0230)$  (°C) is surface soil temperature, and  $T_{a \text{ min}}$  (°C) is the minimum air temperature obtained from the nearest National Weather Service station. For the 1330 LST measurement, surface soil temperature was related to apparent canopy temperature and an exponential function of percent cover (PC). The equation

$$T_s(1330) = 0.79 T_c(1330) \times e^{(-0.80 \text{ PC})} + 20.35 \quad (3)$$

with an  $r^2$  of 0.86 was obtained where PC is expressed as a fraction.

Equations (1), (2), and (3) were tested using simulated HCMM data (aircraft thermal scanner data collected at an altitude of 3650 m AGL) collected over corn, soybean, millet, and pasture (Heilman and Moore, 1979a). Percent canopy cover ranged from 50 to 80 percent for pasture and from 90 to 95 percent for corn, soybean, and millet. Soil textures ranged from sandy loam to silty clay loam.

Figure 3 compares observed soil water content with values predicted using equations (1) through (3) and simulated HCMM measurements of apparent canopy temperature. Equation (1) was converted to express soil water content as a percent field capacity to minimize textural differences (Schmugge et al., 1978). The average difference of observed from predicted values was 1.6 percent of field capacity.

Preliminary analyses of actual HCMM data of eastern South Dakota indicates that high soil moisture areas can be detected using HCMM thermal imagery. In early April 1978 heavy spring runoff and ice blockage caused significant flooding of alluvial areas in a portion of the Big Sioux River Basin in southeastern South Dakota (Fig. 4). Flood waters had receded by mid-May, but an area of high soil moisture (at or near field capacity) remained. Soil moisture in the surrounding upland soils was generally less.

The high moisture area appeared cooler than surrounding areas on May 15 day thermal imagery (Fig. 5). Temperature differences between the flood plain and surrounding areas were probably the result of thermal inertia and evaporation differences associated with soil moisture differences. The high moisture area was not visible on Landsat imagery (Fig. 6) which confirms that no standing water was present in the fields. Adjacent alluvial areas did not appear different from uplands, indicating that the anomaly was not associated with inherent thermal inertia of the soil but with a moisture difference.

These results indicate a potential for evaluating soil moisture using HCMM data. Final results from HCMM soil moisture investigations currently in progress will continue to evaluate the utility of using HCMM and similar data for quantifying soil moisture difference from space.

#### Groundwater

Surface soil temperatures are controlled not only by meteorological factors and soil/water/vegetation properties at depths within the diurnal damping depth, but also by the ability of underlying soil material to store and transfer heat. For example, the high heat capacity of groundwater within the depth of annual soil temperature variation produces a heat sink in summer and a heat source in winter which reduces annual temperature variations (Cartwright, 1968). Variations in groundwater depth do not significantly affect the amplitude of the diurnal temperature curve, but do shift the curve up or down in absolute magnitude (Huntley, 1978).

Figure 7 illustrates the effect of depth to groundwater on subsurface soil temperatures measured in the Big Sioux River Basin in southeastern South Dakota. A highly significant positive correlation ( $r = 0.68^{**}$ ) was found between 50-cm soil temperature and depths to groundwater of three meters or less.

Myers and Moore (1972) and Moore and Myers (1972) evaluated aerial thermography of the Sioux Basin and found that apparent thermal anomalies related to shallow groundwater could be detected during

predawn hours in August and early September, the period of the maximum downward temperature gradient in South Dakota (Fig. 8). In addition, they found that the thickness of saturated sands and gravels corresponded closely to an apparent cool anomaly. During the daytime, they found that thermal patterns produced by differential ET rates, ground shadings, reflectances, and other factors masked thermal patterns produced by subsurface conditions (Fig. 8).

Similar results are visible on HCMM imagery. The Big Sioux Basin appears cooler than surrounding areas on August night thermal imagery, primarily because of the heat sink created by shallow aquifers within the Basin (Fig. 9). The Big Sioux Basin is not visible on day thermal or visible imagery because of the masking effect associated with land use (Figs. 10 and 11). Investigations are in progress to evaluate HCMM and similar data for evaluating depth to groundwater for the shallow water tables.

#### DISCUSSION

Although the potential for using HCMM and similar data in soil moisture and groundwater investigations has been demonstrated, there are limitations in the use of such data which must be considered. Environmental factors which influence energy balance interactions must be considered when using thermal data. Due to its large heats of fusion and vaporization, water undergoing phase transformations act as a heat source or sink. Changes in heat content will not be represented by a corresponding temperature change if a phase transformation

occurs. Thus, conditions favoring high ET rates or dew or frost formation are not favorable for remote sensing of shallow groundwater or for assessing near-surface soil moisture.

Soil moisture and shallow groundwater affect surface temperature in the same direction during the day, and in opposite directions at night during the later-summer period of maximum downward temperature gradients. Thus, thermal inertia and heat sink interactions must be considered, particularly in groundwater investigations.

Wind patterns may obscure thermal anomalies created by soil moisture and groundwater (Fig. 12). Topographic variations and vertical extrusions affect the boundary layer and thus affect sensible and latent heat transport.

Atmospheric constituents (clouds, aerosols, water vapor, etc.) influence surface temperature by attenuating incoming solar radiation and affecting radiative cooling of the surface. Since atmospheric counter-radiation is emitted by atmospheric constituents, radiative cooling will be greater under a clear sky. Atmospheric components also affect the amount of longwave radiation emitted by the surface that is detected by HCMM or other thermal sensors.

Thermal remote sensing has an advantage of relating to subsurface properties since surface temperatures and emittances are a function of both surface and subsurface properties. These preliminary results indicate that observations at appropriate periods within the diurnal cycle can provide information on soil moisture. Observations at appropriate

periods of the diurnal and annual temperature cycle may reveal information on shallow water tables within the range of the annual damping depth (10 to 15 m in northern latitudes of South Dakota). These and other preliminary results appear promising for development of interpretation models to advance the use of thermography.

#### ACKNOWLEDGMENTS

Partial support for the investigations was provided by NASA under contract No. NAS5-24206, USGS under contract No. 14-08-0001-12510, and the State of South Dakota. Contribution No. SDSU-RSI-J-79-12 from the Remote Sensing Institute, South Dakota State University.

## LITERATURE CITED

- Cartwright, K. 1968. Temperature prospecting for shallow glacial and alluvial aquifers in Illinois. Illinois State Geological Survey Circular 433, Urbana, Illinois.
- Heilman, J.L., and D.G. Moore. 1979a. Thermography for estimating near-surface soil moisture under developing crop canopies. J. Appl. Meteor. (accepted).
- Heilman, J.L., and D.G. Moore. 1979b. HCMM detection of high soil moisture areas. Remote Sensing Environ. (submitted).
- Huntley, D. 1978. On the detection of shallow aquifers using thermal infrared imagery. Water Resour. Res. 14:1075-1083.
- Idso, S.B., T.J. Schmugge, R.D. Jackson, and R.J. Reginato. 1975. The utility of surface temperature measurements for the remote sensing of surface soil water status. J. Geophys. Res. 80:3044-3049.
- Idso, S.B., R.D. Jackson, and R.J. Reginato. 1976. Compensating for environmental variability in the thermal inertia approach to remote sensing of soil moisture. J. Appl. Meteor. 15:811-817.
- Moore, D.G., and V.I. Myers. 1972. Environmental factors affecting thermal groundwater mapping. Interim report RSI-72-06 to USGS. Contract No. 14-08-0001-12510, Washington, D.C.
- Myers, V.I., and D.G. Moore. 1972. Remote sensing for defining aquifers in glacial drift. Proc. of 8th International Symp. of Remote Sensing of Environment, Ann Arbor, Michigan. pp. 715-728.
- Schmugge, T., B. Blanchard, A. Anderson, and J. Wang. 1978. Soil moisture sensing with aircraft observations of the diurnal sensing with aircraft observations of the diurnal range of surface temperature. Water Resour. Bull. 14:169-178.

LIST OF FIGURES

- Fig. 1. An August 29, 1978, night HCMM thermal infrared image (scene ID A-A0125-08340) of portions of the upper Midwest. (Approximate scale 1:4,000,000, dark is cool).
- Fig. 2. Relationship of the difference ( $\Delta T_s$ ) between soil surface temperatures measured at HCMM overpass times and the average 24-hr volumetric soil water content (SWC) in the 0 to 4-cm layer of the profile. Temperatures were measured by thermocouple 1 mm below the surface in a field of Volga loam (Heilman and Moore, 1979a).
- Fig. 3. Comparison of predicted and observed values of 24-hr average soil water content in the 0 to 4-cm layer of the soil profile. Predictions were made using equations (1), (2), and (3) and simulated HCMM measurement of canopy temperature (Heilman and Moore, 1979a).
- Fig. 4. Landform map of Brookings County, South Dakota, showing location of alluvial soils (bottomland) in the Big Sioux River Basin which were flooded in early April 1978 (Heilman and Moore, 1979b).
- Fig. 5. Photographic enlargement of a May 15, 1978, day HCMM thermal infrared image (scene ID A-A0029-19575) showing a high soil moisture area in eastern South Dakota (Heilman and Moore, 1979b). Dark is cool.
- Fig. 6. Photographic enlargement of a May 13, 1978, Landsat MSS7 image (scene ID E-21207-16083) of the same area shown in Fig. 5. (Heilman and Moore 1979b).
- Fig. 7. Relationship of 50-cm soil temperatures of depth to groundwater for row crops and pasture. Temperatures were measured in the Big Sioux River Basin during daylight hours on September 5-7, 1978.
- Fig. 8. Day and night thermal imagery of the Sioux Basin north of Sioux Falls. The night image (b) shows a broad cool pattern within the flood plain associated with subsurface conditions. Daytime (a) thermal patterns mask anomalies associated with subsurface conditions. The flood plain is delineated by the dotted line; numbers are thickness (m) of saturated sands and gravels. Approximate scale 1:60,000, dark is cool. (After Moore and Myers, 1972; Myers and Moore, 1972).
- Fig. 9. Photographic enlargement of an August 29, 1978, night HCMM thermal infrared image (scene ID A-A0125-08340) showing the Big Sioux Basin. Note that the Basin appears cooler than surrounding areas, due primarily to the heat sink produced by shallow groundwater within the Basin. (Approximate scale 1:1,000,000; dark is cool).

- Fig. 10. A September 4, 1978, photographic enlargement of a HCMM day thermal infrared image (scene ID A-A0131-19420) of the same area shown in Fig. 9. Note that the Big Sioux River Basin is not visible because of emittance variation associated with land use. (Approximate scale 1:1,000,000; dark is cool).
- Fig. 11. A September 4, 1978, positive photographic enlargement of a HCMM day visible image of the same area shown in Fig. 9 and 10. Note that the Big Sioux River Basin is not visible. (Approximate scale 1:1,000,000).
- Fig. 12. Wind patterns on night thermal imagery of an area south of and including Sioux Falls. Wind was from the northeast at a speed of 10 knots. Approximate scale 1:55,000; dark is cool.

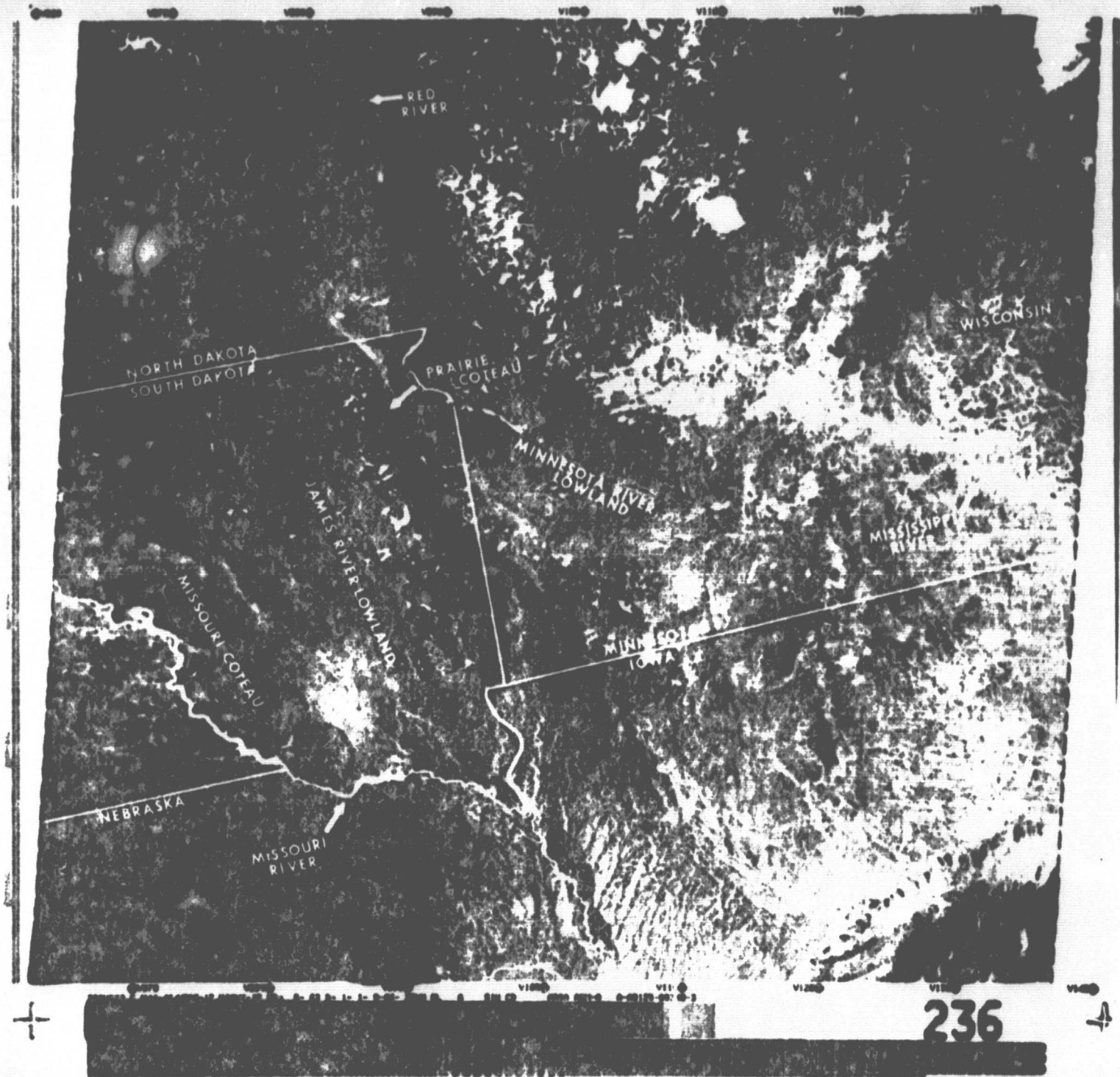


Fig. 1. An August 29, 1973, night HCM thermal infrared image (scene ID A-A0125-08340) of portions of the upper Midwest. (Approximate scale 1:4,000,000, dark is cool).  $ne\Delta T = 0.4^{\circ}C$ ; IFOV = 0.6 x 0.6 km; overpass time = 0234 local standard time.

ORIGINAL PAGE IS  
 OF POOR QUALITY

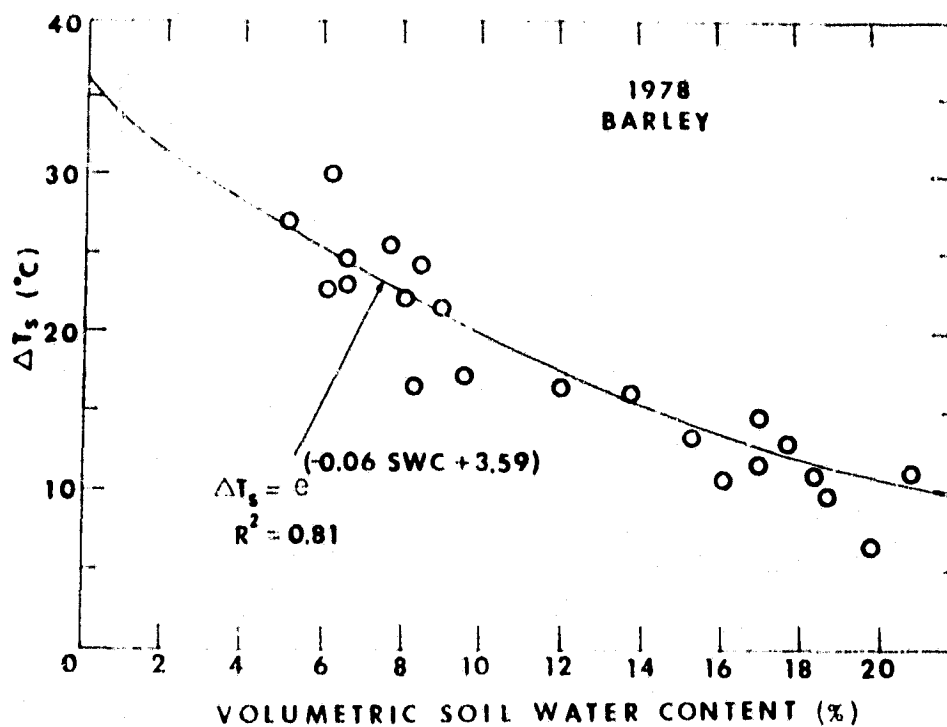


Fig. 2. Relationship of the difference ( $\Delta T_s$ ) between soil surface temperatures measured at HCMM overpass times and the average 24-hr volumetric soil water content (SWC) in the 0 to 4-cm layer of the profile. Temperatures were measured by thermocouple 1 mm below the surface in a field of Volga loam (Heilman and Moore, 1979a).

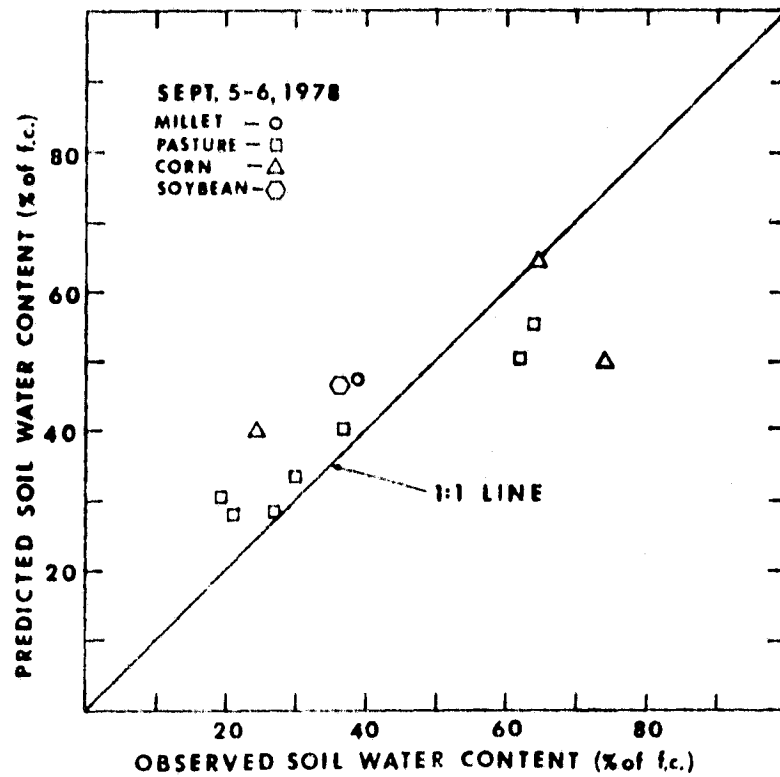


Fig. 3. Comparison of predicted and observed values of 24-hr average soil water content in the 0 to 4-cm layer of the soil profile. Predictions were made using equations (1), (2), and (3) and simulated HCMM measurement of canopy temperature (Heilman and Moore, 1979a).

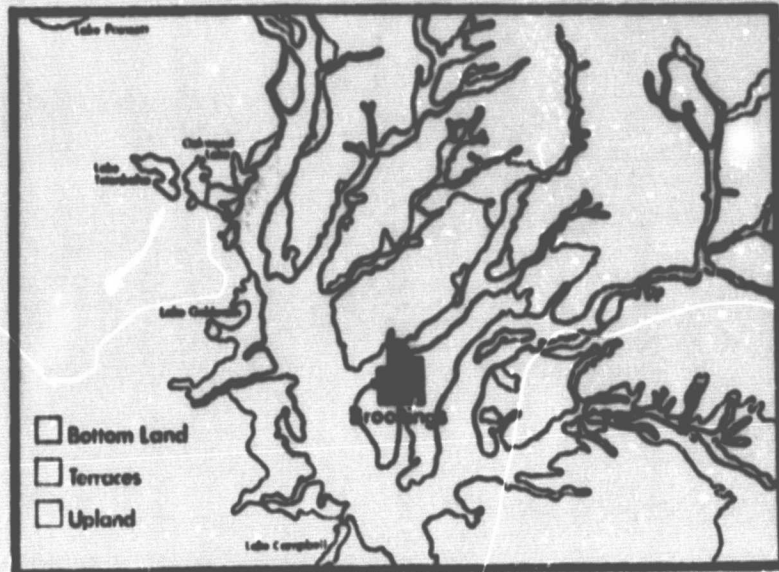


Fig. 4. Landform map of Brookings County, South Dakota, showing location of alluvial soils (bottomland) in the Big Sioux River Basin which were flooded in early April 1978 (Heilman and Moore, 1979b).

ORIGINAL PAGE IS  
OF POOR QUALITY

ORIGINAL PAGE IS  
OF POOR QUALITY



Fig. 5. Photographic enlargement of a May 15, 1978, day HCMM thermal infrared image (scene ID A-A0029-19575) showing a high soil moisture area in eastern South Dakota (Heilman and Moore, 1979b). Dark is cool.

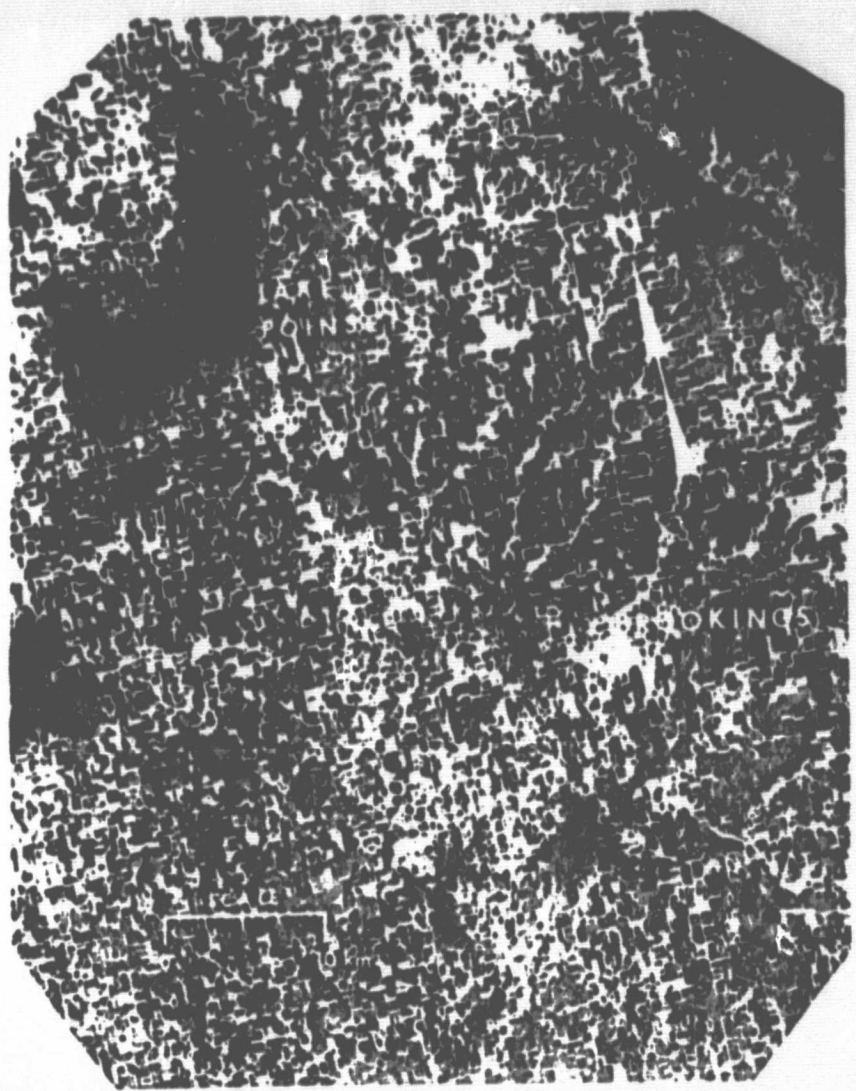


Fig. 6. Photographic enlargement of a May 13, 1978, Landsat MSS7 image (scene ID E-21207-16083) of the same area shown in Fig. 5. (Heilman and Moore, 1979b).

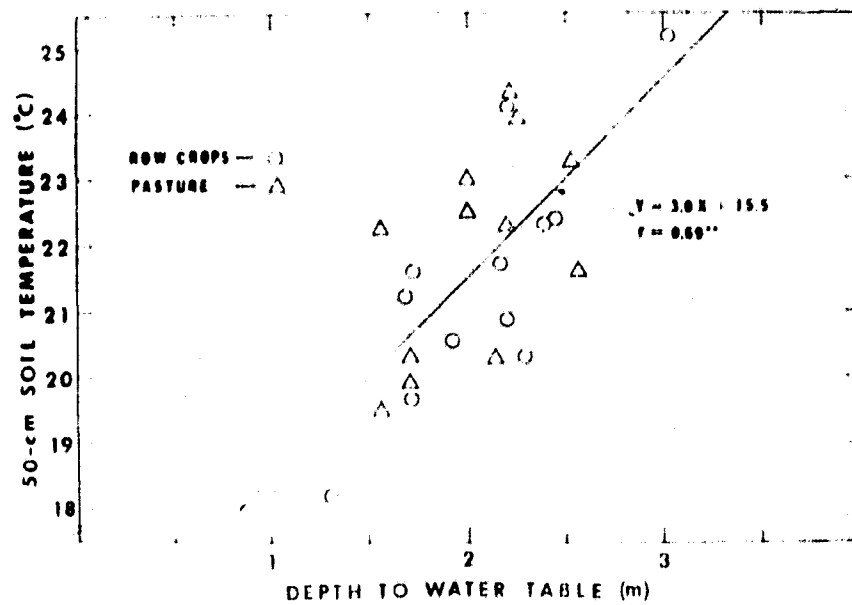
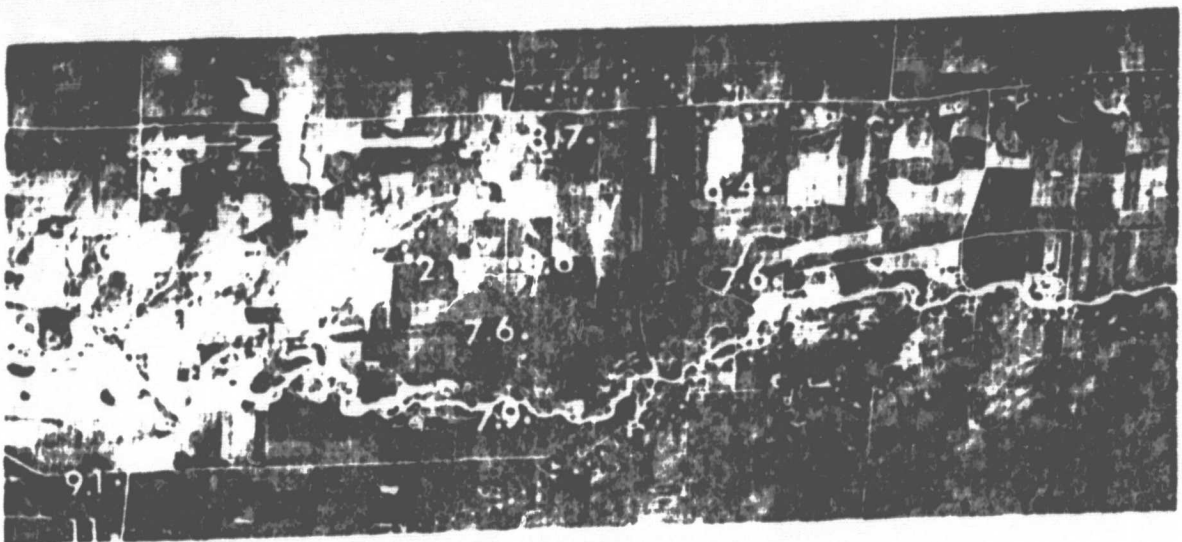


Fig. 7. Relationship of 50-cm soil temperatures of depth to ground-water for row crops and pasture. Temperatures were measured in the Big Sioux River Basin during daylight hours on September 5-7, 1978.



a DAY, AUGUST 28, 1971

ORIGINAL PAGE IS  
OF POOR QUALITY



b NIGHT, AUGUST 26, 1971

Fig. 8. Day and night thermal imagery of the Sioux Basin north of Sioux Falls. The night image (b) shows a broad cool pattern within the flood plain associated with subsurface conditions. Daytime (a) thermal patterns mask anomalies associated with subsurface conditions. The flood plain is delineated by the dotted line; numbers are thickness (m) of saturated sands and gravels. Approximate scale 1:60,000, dark is cool. (After Moore and Myers, 1972; Myers and Moore, 1972).

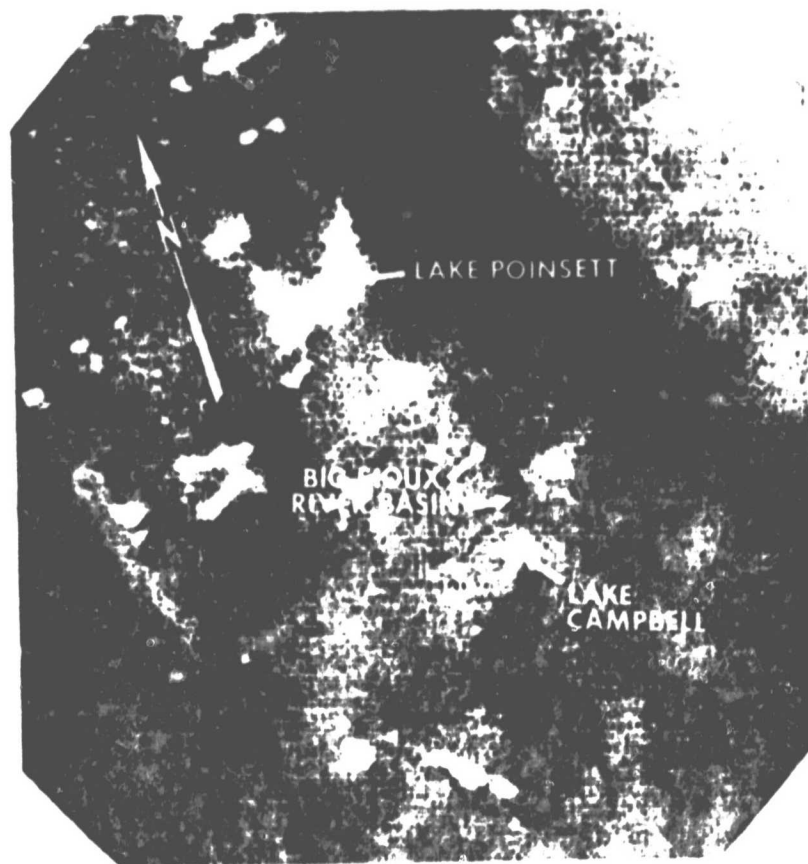


Fig. 9. Photographic enlargement of an August 29, 1978, night HCMM thermal infrared image (scene ID A-A0125-08340) showing the Big Sioux Basin. Note that the Basin appears cooler than surrounding areas, due primarily to the heat sink produced by shallow groundwater within the Basin. (Approximate scale 1:1,000,000; dark is cool).

ORIGINAL PAGE IS  
OF POOR QUALITY

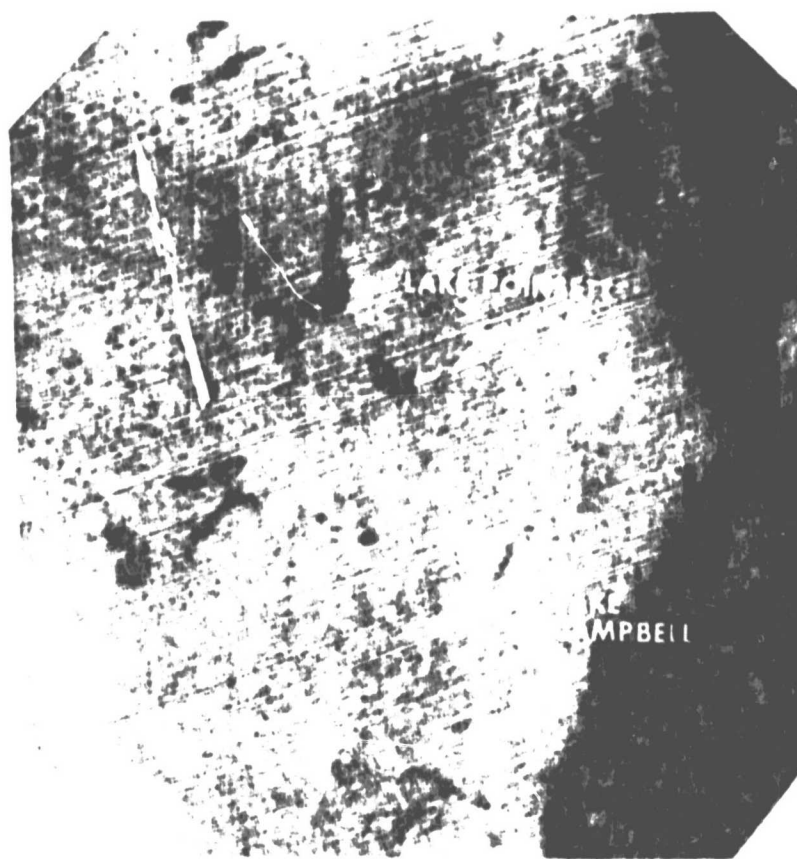


Fig. 10. A September 4, 1978, photographic enlargement of a HCMM day thermal infrared image (scene ID A-A0131-19420) of the same area shown in Fig. 9. Note that the Big Sioux River Basin is not visible because of emittance variation associated with land use. (Approximate scale 1:1,000,000; dark is cool).

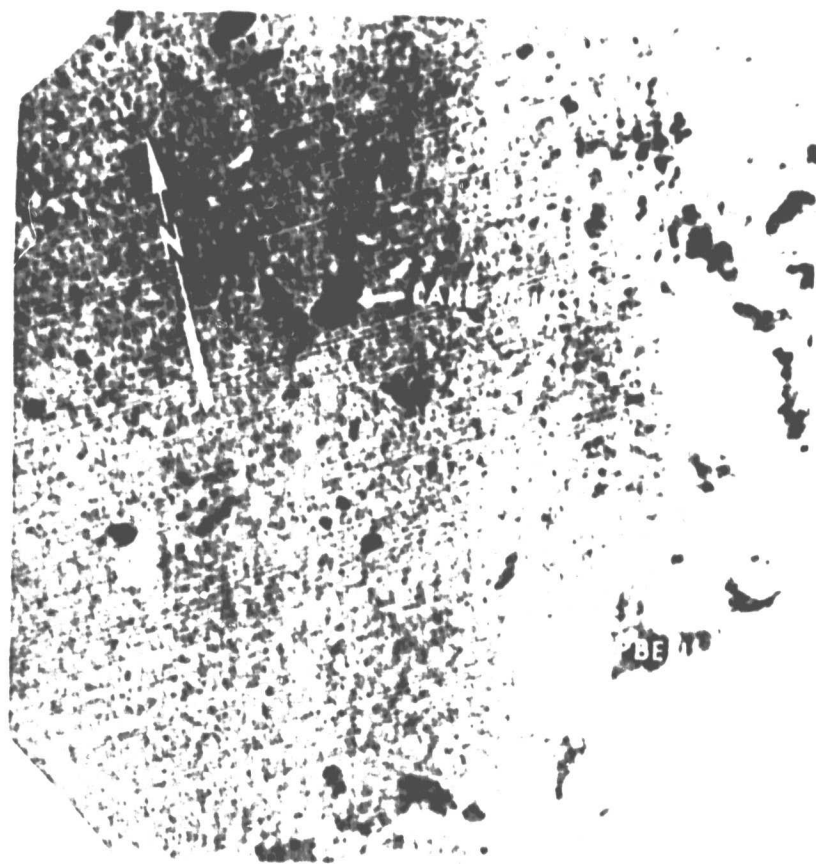


Fig. 11. A September 4, 1978, positive photographic enlargement of a HCMM day visible image of the same area shown in Fig. 9 and 10. Note that the Big Sioux River Basin is not visible. (Approximate scale 1:1,000,000).

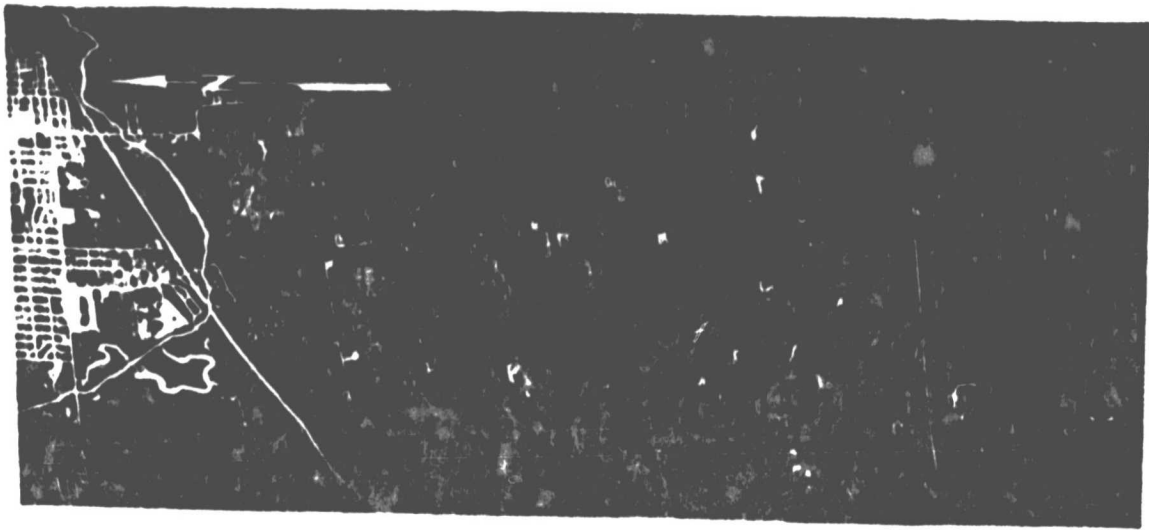


Fig. 12. Wind patterns on night thermal imagery of an area south of and including Sioux Falls. Wind was from the northeast at a speed of 10 knots. Approximate scale 1:55,000; dark is cool.

ORIGINAL PAGE IS  
OF POOR QUALITY